# WELDING RESEARCH

SUPPLEMENT TO THE *WELDING JOURNAL*, DECEMBER 1991

**Sponsored by the American Welding Society and the Welding Research Council**




# A Study Concerning Intercritical HAZ Microstructure and Toughness in HSLA Steels

*Two steels, although similar in composition, proved to have marked differences in intercritical HAZ toughness*


**BY D. P. FAIRCHILD, N. V. BANGARU, J. Y. KOO, P. L. HARRISON AND A. OZEKCIN**



ABSTRACT. Small islands of high-carbon, martensite-austenite (M-A) constituent can form in two heat-affected zone (HAZ) regions of structural steels; the intercritical HAZ (ICHAZ) and the intercritically reheated coarse-grain HAZ (IRCG). Previous work has shown that these islands can reduce toughness in the IRCG; however, in the present study, toughness reduction in the ICHAZ occurred. Two microalloyed HSLA steels were welded by the submerged arc process and ICHAZ toughness was assessed using the Charpy and crack tip opening displacement (CTOD) tests. Optical, scanning electron (SEM), and transmission electron microscopy (TEM) were used to study base metal and ICHAZ microstructure.

One of the steels suffered severe toughness degradation in the ICHAZ as measured by the CTOD test. It was determined by TEM that the only significant low-toughness feature in the ICHAZ was the presence of M-A islands. The formation of the M-A was believed to be caused by a high amount of vanadium and silicon in solid solution, which increased hardenability.

The Charpy data showed no difference between the ICHAZ toughnesses of the steels; whereas, the CTOD results showed a distinct difference. Charpy testing may be insensitive when the microstructure varies over small distances, as is the case for weld HAZs.



*D. P. FAIRCHILD is with the Department of Welding Engineering, The Ohio State University, Columbus, Ohio. N. V. BANGARU is with The Ferrous Wheel Group, Annandale, N.J. J. Y. KOO is with Pohang Iron & Steel Co., Ltd., Pohang City, South Korea. P. L. HARRISON is with British Steel Corp., Moorgate, Rotherham, U.K. A. OZEKCIN is with Exxon Research and Engineering Co., Annandale, N.J.*



**KEY WORDS**

HSLA Steels
Microalloying
Intercritical HAZ
HAZ Transformation
Hardenability
M-A Constituent
Electron Microscopy
HAZ Toughness
CTOD Testing
Charpy Testing


## Introduction

Previous work has shown that low fracture toughness can exist in the coarse-grained HAZ (CGHAZ) of some high-strength low-alloy (HSLA) steels (Refs. 1–6). The low toughness is caused by certain microstructural features, one being identified as islands of high-carbon, martensite-austenite (M-A) constituent in which the martensite has a twinned substructure. The M-A is located in a relatively continuous path along prior austenite grain boundaries (Refs. 2, 7). The M-A is primarily a result of intercritical reheating, which is produced by a subsequent weld pass. Specifically, the M-A is located in a subarea of the CGHAZ called the intercritically reheated coarse-grained HAZ (IRCG) (Ref.1). Various HAZ regions are identified in Fig. 1.

While the intercritical thermal cycle can produce M-A in the IRCG, it is also possible that M-A islands can be created in the intercritical HAZ (ICHAZ) itself. In multipass welds, these are the ICHAZ areas that are unaffected by subsequent

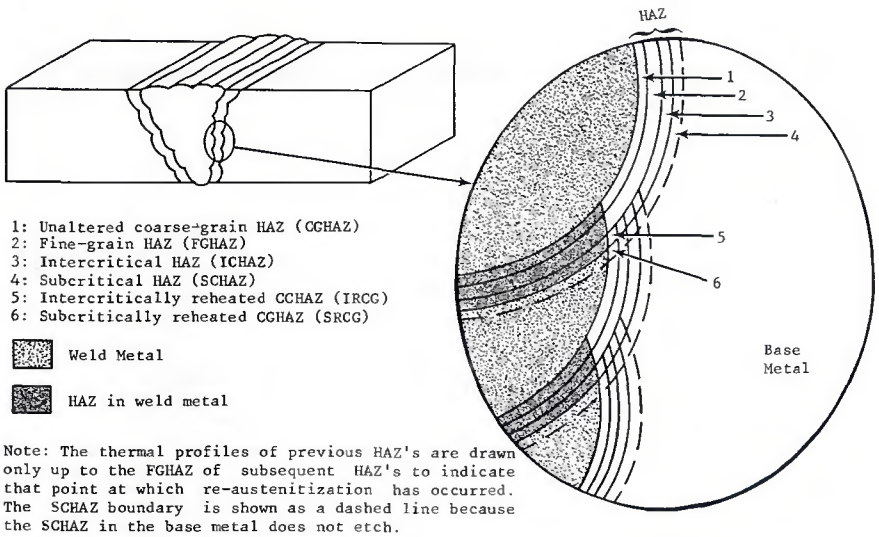


*Fig. 1 — Various HAZ regions in a multipass weld.*

weld passes. The ICHAZ forms during peak temperature heating between approximately 727°C (1341°F) and 850°C (1562°F) — Fig. 2. The low-temperature boundary of the ICHAZ is the $Ac_1$, and the high-temperature boundary is the $Ac_3$.

Uchino and Ohno (Ref. 8) report finding low-ICHAZ toughness in experimental heats of HSLA steels. They produced ICHAZ microstructures by thermal simulation, and measured toughness using the Charpy test. The low toughness was caused by M-A islands, and the volume fraction of the M-A increased with vanadium content.

This paper documents a study concerning ICHAZ toughness in two commercial HSLA steels. While the steels have subtle differences in composition, they have marked differences in ICHAZ toughness. Multipass welds were produced using the submerged arc process. Charpy and crack-tip opening displacement (CTOD) tests were conducted to assess toughness. Base metal and ICHAZ microstructures were studied using optical, scanning electron (SEM), and transmission electron microscopy (TEM).

## Experimental Procedures

### Materials

Table 1 lists the chemical compositions of the materials used. Both steels were 50 mm (2 in.) thick, normalized, calcium-treated and commercially manufactured to meet BS 4360 Grade 50E specifications. The total microalloy content for both steels was 0.08 wt-%. Steel A contained 0.06 wt-% vanadium and 0.019 wt-% niobium, while steel B contained 0.08 wt-% vanadium. Mechanical property data for these materials are given in Table 2. The Charpy test procedures used for the base metal were consistent with those used for the ICHAZ and are described below.

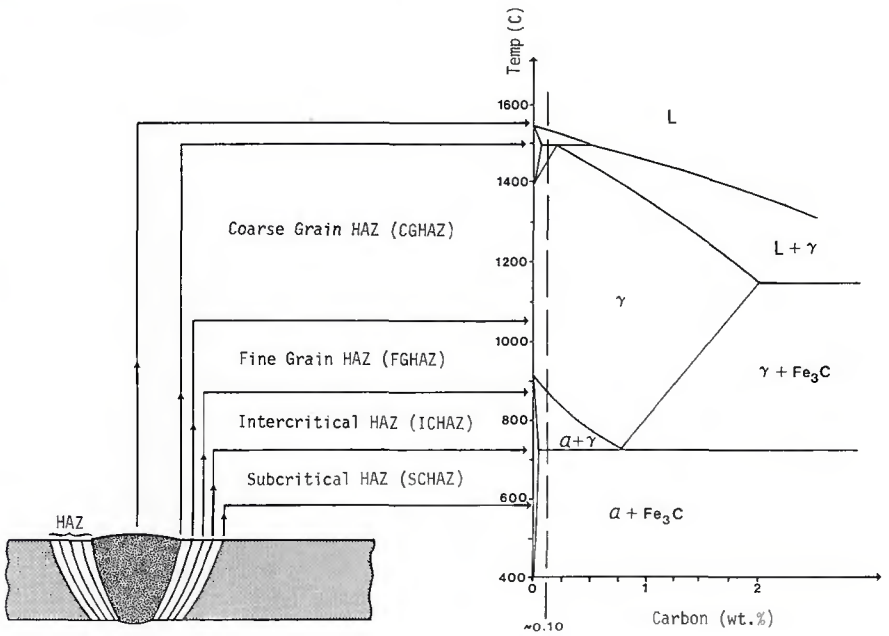


*Fig. 2 — HAZ regions superimposed on the iron-carbon phase diagram.*

### Welding

To produce specimens for toughness testing, a single-V edge preparation was used. The ICHAZ along the square edge of the single-V preparation was the focus for toughness testing. Figure 3 schematically shows the weld geometry and the ICHAZ regions are depicted in solid black. The ICHAZs form a somewhat continuous path from one plate surface to the other. It was desired that the line of ICHAZ areas along the square edge be as straight as possible and perpendicular to the plate surface. These features allow adequate fatigue crack sampling of the desired microstructure when the through-thickness notch orientation is used for CTOD testing (Ref.9). In order to accomplish the desired ICHAZ geometry, a special weld procedure was developed and is detailed in Fig. 4. The heat input for welding was 3 kJ/mm (75 kJ/in.).

To provide specimens for metallurgical evaluation, single-pass bead-in-groove welds were made using parameters identical to those listed in Fig. 4.

### Toughness Testing

Charpy and CTOD tests were conducted with the notch (fatigue crack for CTOD specimens) located in the through-thickness orientation as shown schematically in Fig. 5. It was intended that the root of the notch be positioned directly in the ICHAZ. Approximately ten Charpy tests were conducted for each Steel at various temperatures to determine the transition curve. The values of the 35 J (26 ft-lb) and 50 J (37 ft-lb) transition temperatures are listed in Table 3. The 35-J or 50-J transition temperature is the temperature corresponding to the point on the transition curve whose energy value is 35 J or 50 J, respectively.

Three CTOD tests were conducted for the ICHAZ of each steel And the results are listed in Table 3. The CTOD tests were conducted according to BS 5762. The B X 2B geometry was used, the crack depth was 50% of the specimen thickness, and the test temperature

**Table 1—Chemical Composition (wt-%)**

| Material | C | S | P | Si | Mn | Ni | Cr | Mo | Cu | V | Nb | Ti | Al | N |
|---|---|---|---|---|---|---|---|---|---|---|---|---|---|---|
| Steel A | 0.14 | 0.004 | 0.012 | 0.24 | 1.43 | 0.24 | 0.04 | ND | 0.01 | 0.06 | 0.019 | 0.005 | 0.018 | 0.0078 |
| Steel B | 0.10 | 0.011 | 0.015 | 0.46 | 1.42 | 0.28 | 0.05 | ND | 0.20 | 0.08 | ND[a] | ND[a] | 0.060 | 0.0057 |

(a) ND = not detected (< 0.005).

was –10°C (14°F). After the completion of each test, the specimens were sectioned, polished and etched to ensure that the proper microstructure (*i.e.*, the ICHAZ) was sampled by the fatigue crack.

### Microstructural Analysis

Although some optical work was conducted, the base materials and the ICHAZs were primarily examined using SEM and TEM. The optical and SEM techniques were relatively routine; therefore, only the TEM procedures will be briefly outlined. In order to ensure that the narrow ICHAZ region was in the vicinity of the small hole produced by electropolishing, careful preparation of the HAZ specimen was necessary before punching the 3-mm disk. One side of the sample was polished/etched and the location of interest marked. Then the sample was mechanically thinned to a thickness of 0.005–0.006 in. (0.127–0.152 mm) by grinding from the unmarked side. At this stage the 3-mm disk was punched out making sure that the marked region remained at the center. This procedure maximized the chances of making the ICHAZ region electron transparent. The disks were twin-jet electropolished using an electrolytic solution consisting of 300 mL of methanol, 175 mL of butynol, and 30 mL of perchloric acid. The polishing was done at –40°C. All of the thin foils were examined in a Philips EM 430 microscope at an accelerating voltage of 300 kV. The microscope was equipped with an EDAX detector (20-deg take-off angle) and a 5500 EDAX analyzer. The TEM procedures included dark-field, bright-field, microdiffraction and EDS analysis.

**Table 2—Mechanical Properties**

| | Transverse Tensile Test Data | | | | Transverse Charpy Data at ½ thickness | |
|---|---|---|---|---|---|---|
| Material | Yield Strength (MPa) | Tensile Strength (MPa) | Elongation (%) | Reduction of Area (%) | 35 J[a] (°C) | 50 J[a] (°C) |
| Steel A | 362 | 518 | 29 | 71 | –80 | –75 |
| Steel B | 306 | 506 | 28 | 70 | –90 | –85 |

(a) These values refer to the 35 J or 50 J transition temperature.

## Results

### Charpy and CTOD Data

The Charpy data indicate that the ICHAZ for both steels incurred a reduction in toughness from that of the base metal; the 35-J and 50-J transition tem-

**Table 3—ICHAZ Toughness Data**

| | Charpy Tests | | |
|---|---|---|---|
| Material | 35 J[a] (°C) | 50 J[a] (°C) | CTOD Tests (mm) |
| Steel A | –42 | –36 | 2.02, 1.99, 1.75 |
| Steel B | –40 | –30 | 0.01, 0.08, 0.03 |

(a) These values refer to the 35 J or 50 J transition temperature.

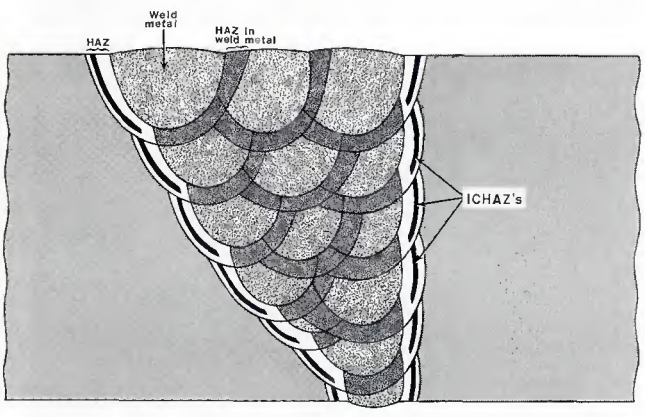


*Fig. 3 — Schematic of weld cross-section showing the location of the intercritical HAZs (ICHAZs).*

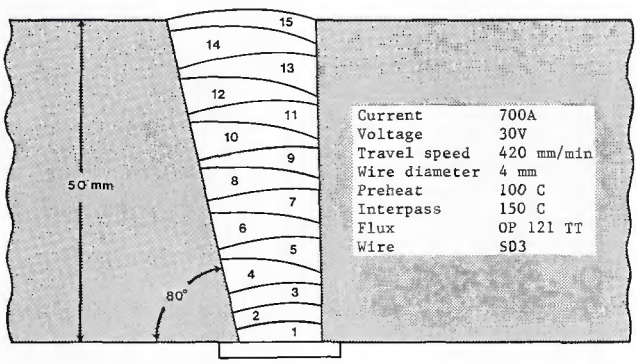


*Fig. 4 — Weld procedure geometry and details.*

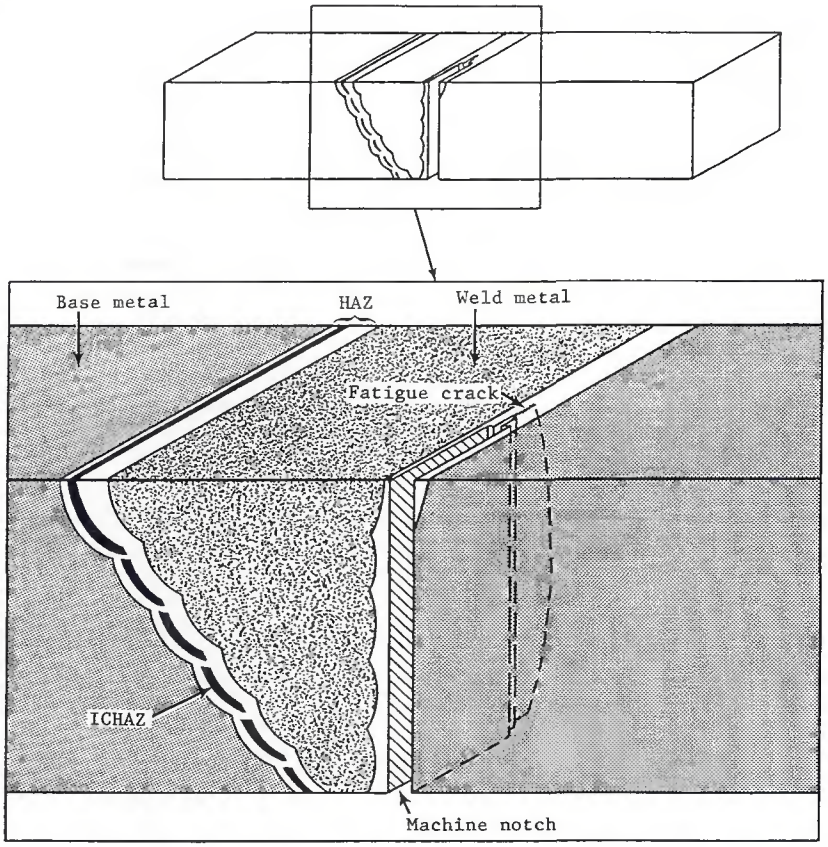


*Fig. 5 — Through-thickness notch orientation for toughness testing.*

**Table 4—HAZ Charpy Requirements from UKDOE Guidance Notes**

| As-Welded Areas of High-Stress Concentration | As-Welded Other Areas |
|---|---|
| 36 J at −40°C | 36 J at −30°C |

peratures increased by about 40°–50°C (72°–90°F). The Charpy data also indicate that the ICHAZ toughness for both steels is essentially the same. Although a loss of toughness was experienced in the ICHAZ, the Charpy values are not drastically low. For comparison purposes, the HAZ Charpy requirements from the UKDOE Guidance Notes (Ref.10) for BS 4360 Grade 50 steel are listed in Table 4. This standard is used for the design and construction of offshore platforms in the U.K. sector of the North Sea, a common application for these steels. The ICHAZ Charpy values for both of these steels meet the required value of 35 J at a test temperature of –40°C (–40°F).

The CTOD values for Steel A indicate that the ICHAZ of this material has high fracture toughness. The CTOD values for Steel B, however, indicate that this material has very low toughness. All values for Steel B are in or near the linear elastic regime (Ref.1) and this is in con-

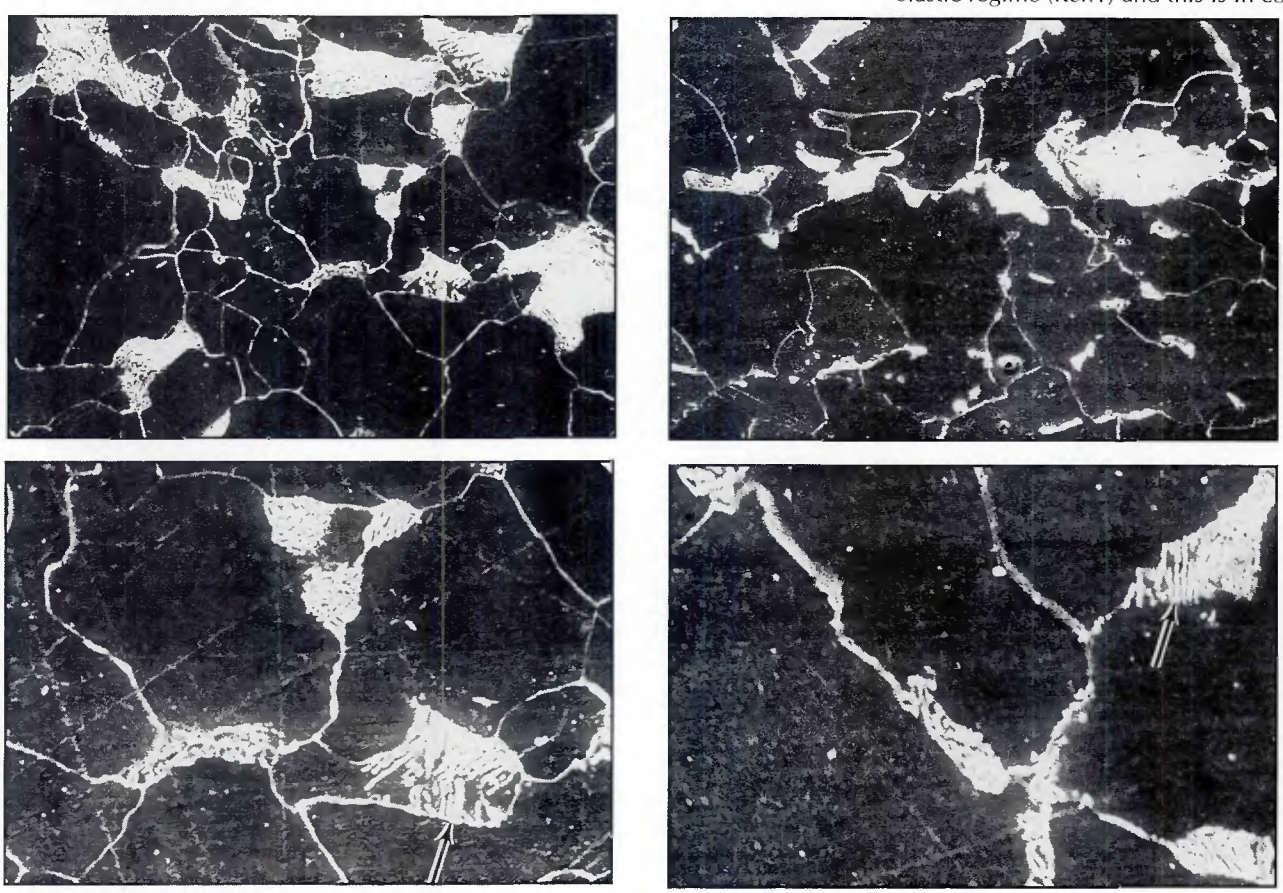

*Fig. 6 — Base metal SEM micrographs of Steels A (left) and B (right). Examples of pearlite are denoted by arrows.*

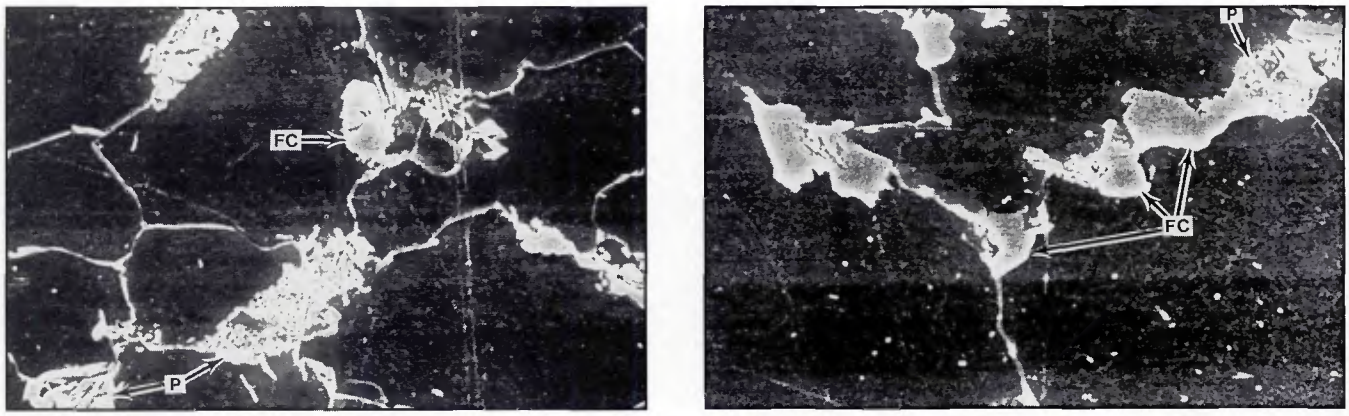


*Fig. 7 — SEM micrographs of the ICHAZ for Steels A (left) and B (right). Examples of pearlite are denoted by "P" and the featureless constituent is denoted "FC."*

tradiction to the Charpy data. Typical required HAZ CTOD values for these steels (Ref. 8) are in the range of 0.15–0.35 mm (0.006–0.014 in.). While Steel A easily meets these required values, Steel B does not.

#### Microstructure — SEM Examined

The base metal microstructures for both steels, as photographed in the SEM at two different magnifications, are shown in Fig. 6. The steels exhibit a ferrite-pearlite microstructure. From observation of several areas of the samples, it was concluded that no detectable difference in the morphology of the pearlite exists in the two steels, although the amount of pearlite in Steel A is somewhat higher due to a higher carbon content. As seen in Fig. 6, Steel A has a slightly smaller grain size than Steel B; 15 microns compared to 20 microns.

Figure 7 shows SEM micrographs of the ICHAZ for the two steels. The difference in grain size is again apparent. Both steels show a primary microstructure of ferrite with second-phase networks (islands) distributed around the ferrite grain boundaries. Considering the relative amounts of the two phases, it is believed that during welding the peak temperature in this region of the ICHAZ was about 780°C (1436°F). It was apparent that the structural makeup of the second phases was different between Steels A and B. In Steel A, the second phase is predominantly pearlite with the remainder being a featureless constituent (featureless at the magnification level afforded by SEM). In Steel B, pearlite comprises only a minor fraction of the second phase, while the major portion is a featureless constituent. Figure 7 shows that the featureless constituent in Steel B is relatively continuous and well connected around the ferrite grain boundaries. TEM analyses were required to determine the nature of the featureless constituent and to observe any microalloy precipitates present in the ferrite.

#### Microstructure — TEM Examined

Figure 8 shows TEM micrographs of the base metal ferrite in both steels. A large number of microalloy precipitates in the ferrite of Steel A are apparent. These precipitates were identified as primarily Nb-V carbonitrides (Nb,V(C,N)). In contrast, the ferrite of Steel B contains few precipitates. The few observed are primarily V-bearing carbonitrides (V(C,N)). Apparently, a significant amount of the V in Steel B is in solid solution in the ferrite matrix.

TEM micrographs of the ferrite phase from the ICHAZ of both steels are shown in Fig. 9. It is clear from this figure that the microalloy precipitates seen in the base metal ferrite of Steel A are also present in the ICHAZ. The ICHAZ ferrite of Steel B is largely void of microalloy precipitates, as was the base metal ferrite. These observations indicate that the microalloy precipitation pattern present in the base metal ferrite survives the ICHAZ thermal cycle.

TEM micrographs of the second phase from the ICHAZ of Steel A are shown in Fig. 10. The predominant second-phase constituent is pearlite (including degenerate pearlite) and is shown in Fig. 10A. The minor con-

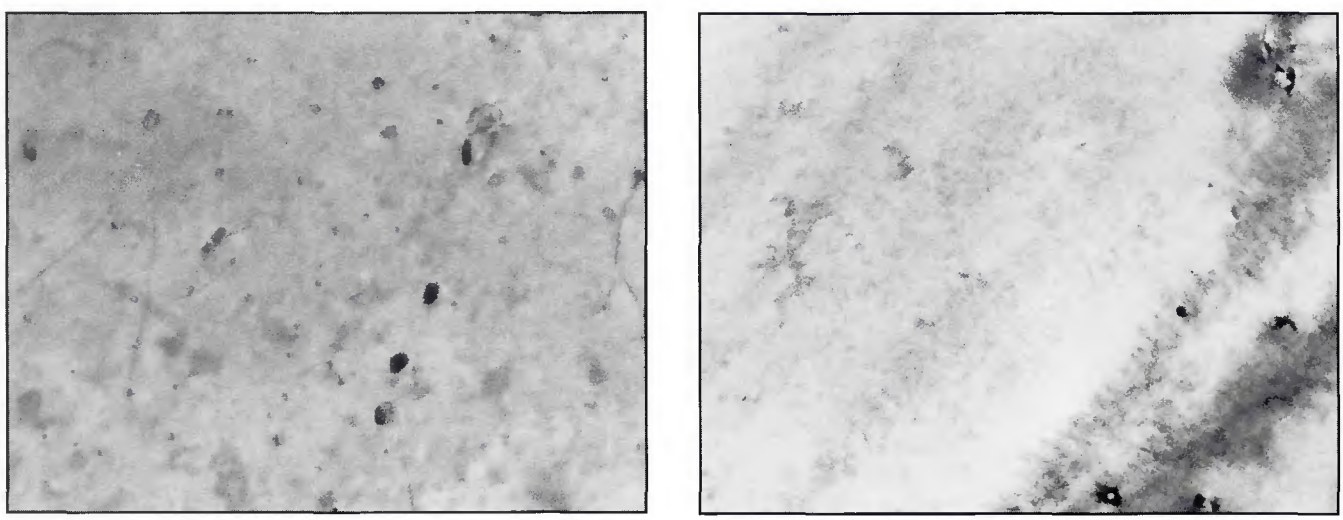

*Fig. 8 — TEM micrographs of the base metal ferrite in Steels A (left) and B (right).*

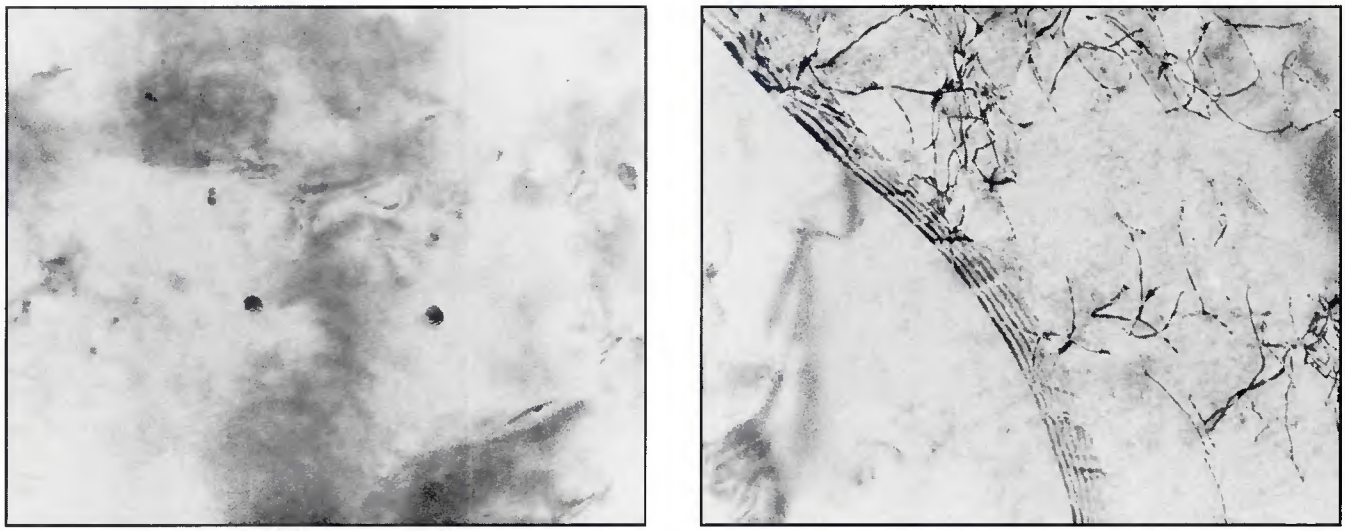

*Fig. 9 — TEM micrographs of the ICHAZ ferrite in Steels A (left) and B (right).*

stituent of the second-phase was identified as mostly upper bainite; however, a small amount of M-A is also present. The upper bainite is shown in Fig. 10B. Figure 10 shows that within the pearlite, the ferrite phase between the cementite plates is relatively dislocation free; whereas, in the bainite, the dislocation density in the ferrite is significant. The presence of this dislocation density indicates that the bainite transformation has a shear component and that the ferrite has been strained.

Figure 11 shows a TEM micrograph of the second phase in the ICHAZ of Steel B. The microstructure is mainly M-A constituent. The martensite is the predominant phase of the M-A constituent comprising about 96 to 97 vol-%. The M-A islands are on the order of 1 to 10 microns in size. The martensite possesses a twinned substructure and this feature is indicative of a high-carbon content; > 0.5% (Ref. 11). This type of M-A constituent is known to be quite brittle. Only a minor fraction of the ICHAZ microstructure in this steel was identified as pearlite.

## Discussion

The difference in fracture toughness between the two steels is caused by the different ICHAZ microstructures. The major difference in the microstructures was in the nature of the second phase: Steel A being primarily pearlitic and Steel B being primarily M-A constituent. To understand how these differences in second-phase microstructure arise, the time-temperature-transformation phenomena occurring in the ICHAZ must be understood.

### Intercritical HAZ Formation

With a base metal microstructure composed primarily of ferrite-pearlite, transformation to austenite begins when the heating portion of the HAZ thermal cycle reaches the eutectoid temperature (727°C/ 1341°F). The first areas to transform to austenite are the regions of pearlite. However, in relatively low-carbon steels, such as used in this study, the volume fraction of pearlite is low and is consumed early in the intercritical range. As the temperature increases, other nucleation sites for the austenite appear, most notably at ferrite-ferrite grain boundaries. Because HAZ thermal cycles are rapid, the temperature may only be in the intercritical range for three to six seconds as shown in Fig. 12 (derived from Ref. 12). For a heat input of 3 kJ/mm (75 kJ/in.) and a peak tempera-

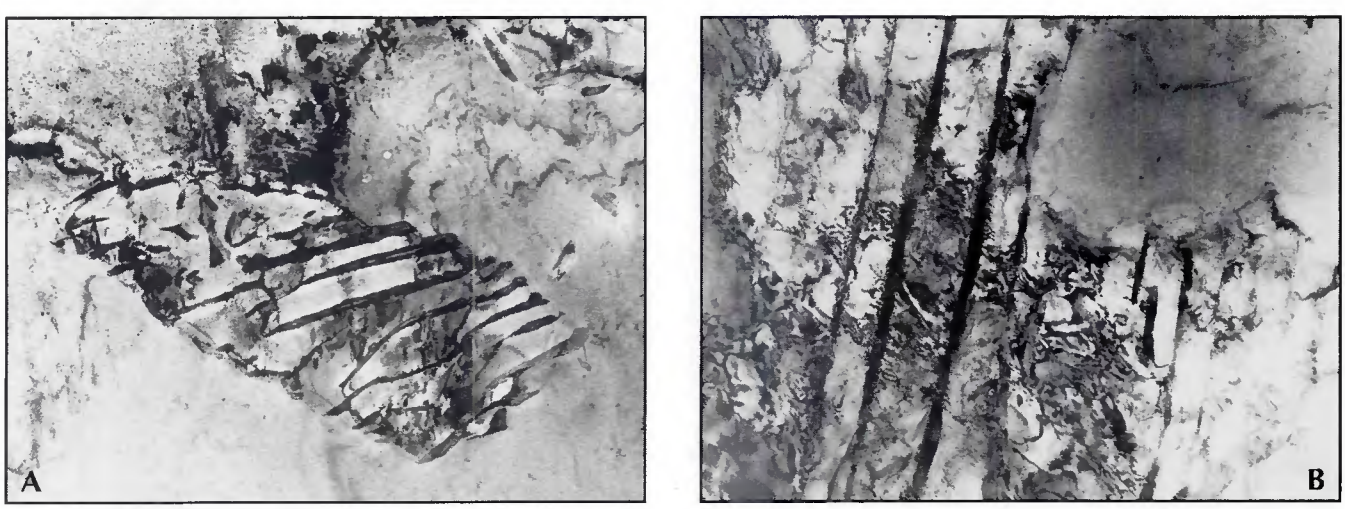


*Fig. 10 — A — TEM micrograph of the predominant ICHAZ second phase in Steel A, pearlite; B — TEM micrograph of the minor ICHAZ second phase in Steel B, upper bainite.*

ture of about 780°C (1436°F), a large number of austenite nucleation sites will develop, but very little growth occurs because cooling begins quickly. The austenite is, therefore, limited to small islands at prior pearlite sites and ferrite-ferrite grain boundaries.

Upon cooling, the austenite islands decompose and become the second-phase of the ICHAZ. The primary phase, the ferrite, is that of the original base metal. The factors that determine the structure that forms from the austenite are the ICHAZ cooling rate and the austenite hardenability. In the present program, both steels experienced identical welding conditions; *i.e.*, the same ICHAZ thermal cycle. Therefore, the difference in second-phase microstructure between Steels A and B is only a factor of austenite island hardenability. Because the second phase of Steel B was that of a lower temperature transformation product, it is believed that the austenite islands possessed higher hardenability than for Steel A.

The difference in the hardenability of the austenite islands (and thus the ICHAZ second phase) is caused by the concentration of microalloying and alloying elements in solid solution. The most notable differences between the two steels with respect to elements that have a significant effect on hardenability are the V, Si, and C content.

*Vanadium.* Ordinarily, microalloying elements do not have a significant effect on hardenability because they are tied up in the form of stable precipitates. This is the case for Steel A where Nb and V are largely in the form of carbonitrides. For Steel B, however, few precipitates were observed in both the base metal and the ICHAZ, and this is evidence that much of the V is in solid solution. The hardenability of steels is greatly enhanced when the microalloying elements (especially V) are in solid solution (Ref. 13). It is interesting that Ref. 8 reports that the volume fraction of M-A increases in simulated ICHAZs with increasing V content.

The reason for the difference in the solid solution microalloy content between the two steels is not precisely known, but some explanations can be offered. Both steels were normalized, and they contained approximately the same total microalloy content. The solubility of Nb(C,N) in austenite is much lower than that of V(C,N). Thus, the mixed Nb,V(C,N) in Steel A may have produced relatively insoluble carbonitrides, while in Steel B, the pure V(C,N) may have readily dissolved during the normalizing treatment. It also appears likely that Steel B experienced a faster cooling rate during its normalizing treatment, which would hinder the formation of microalloy precipitates.

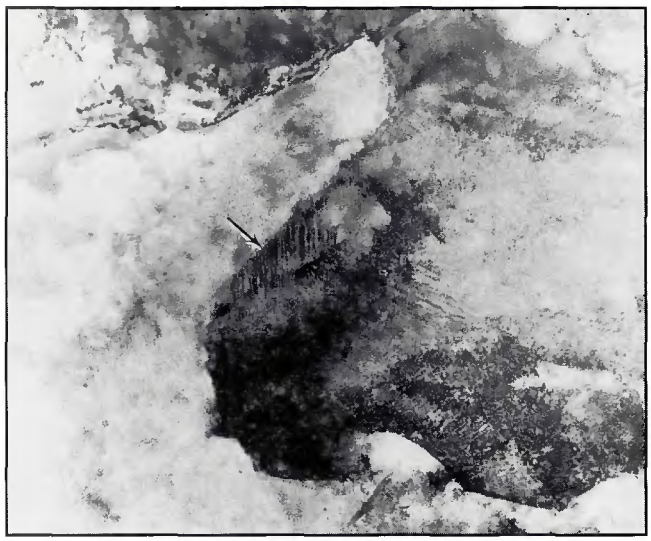

*Fig. 11 — TEM micrograph of the ICHAZ second phase in Steel B showing twinned martensite (arrow) and M-A constituent.*

The specific cause of the microalloy distribution in Steel B is not, however, the focus of attention. The important fact is to realize that the ICHAZ of steel welds can develop undesirable microstructures as a result of the original base metal condition (which is controlled by the steel manufacturing technique). The ICHAZ thermal cycle, unlike that of the CGHAZ, is not of sufficient intensity to eliminate all traces of base metal processing. ICHAZ fracture performance can be significantly affected by the steel manufacturing technique.

*Silicon.* The Si content of Steel B is higher than that for Steel A (0.46 vs. 0.26 wt-%) and is believed to contribute to the difference in austenite island hardenability. It has been shown (Ref. 13) that Si content in the range of 0.5 wt-%, in the presence of a significant amount of V (about 0.08 wt-%), promotes the formation of twinned martensite and M-A constituent during intercritical heating.

*Carbon.* Steel A has a higher carbon content than Steel B (0.14% vs. 0.10%) and this difference is contrary to the theory of higher austenite island hardenability in Steel B. With respect to C content, the chemical analysis results may be slightly misleading. Some of the C in Steel A is tied up in the form of microalloy precipitates and does not affect austenite island hardenability. For Steel B, few precipitates exist; thus, the C (as is the V) is available to increase hardenability. Even considering this C "tie-up" effect, it is likely that Steel A had more C available to influence hardenability than did Steel B. The observed microstructure shows, however, that the difference in C was overcome by the ef-

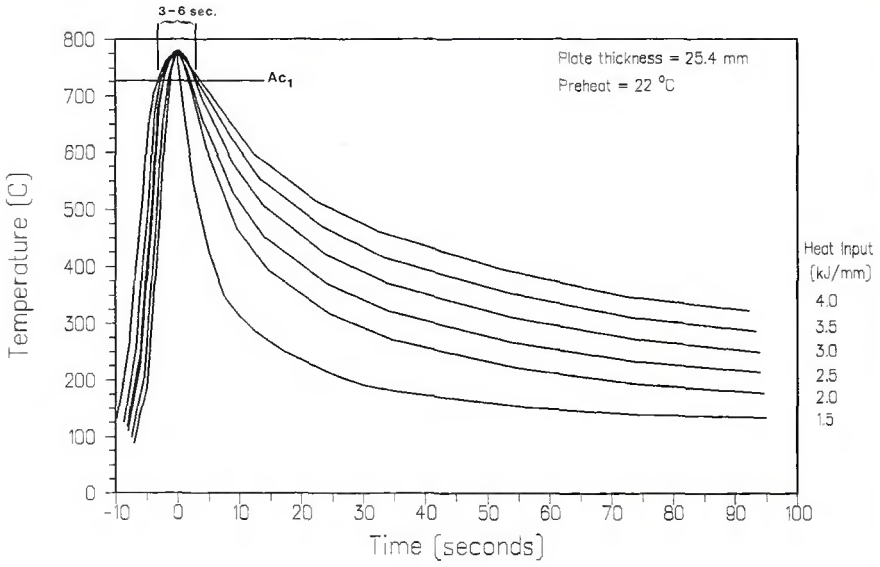


*Fig. 12 — ICHAZ thermal cycles with the time above the $A_{c1}$ highlighted.*

fect of V and Si to the extent that the lower C steel displayed higher austenite island hardenability in the ICHAZ.

Carbon also plays an important role in determining the substructure morphology of any ICHAZ martensite that does form. By referring to Fig. 2 and using the lever rule, it can be seen that during the intercritical portion of the ICHAZ thermal cycle, the austenite islands are enriched in carbon far above the level of the base metal. These enriched islands then experience a relatively rapid cooling rate, which limits carbon mobility and leaves the local carbon content higher than the bulk of the matrix. This enrichment mechanism is responsible for the twinning of the martensite observed in Steel B.

The Cu and Al content was higher in Steel B and while these elements may have had a minor effect on austenite island hardenability they are not believed to be primary factors.

#### The Significance of M-A Islands

While the potential for reduced toughness in structural steel HAZs was realized for decades, only recently have the micromechanisms of fracture initiation in HAZs been studied. A considerable amount of work has concentrated on CGHAZ toughness, specifically the local brittle zone (LBZ) problem (Refs. 1–3, 6, 7, 14). A comparison between the causes of low CGHAZ toughness and low ICHAZ toughness will provide further insight as to the potency of M-A islands for reducing toughness. Before this comparison is made, note that the CTOD values for Steel B in this study and those for low toughness CGHAZs (*i.e.*, for LBZs) are essentially the same: CTOD < 0.10 mm, with some values nearing 0.01 mm (0.0004 in.).

As reported in Ref.1, the metallurgical factors believed to be the main contributors to low-toughness CGHAZs in microalloyed structural steels are as follows:

1) Bulk microstructure of upper bainite.

2) Microalloy precipitation.

3) Large grain size: 75–150 microns (ASTM 5–2).

4) Martensite islands (*i.e.*, M-A constituent).

The relative significance of each factor has not been established. The present study has shown that low ICHAZ toughness in microalloyed steels can be caused by M-A islands alone. In contrast to the CGHAZ features listed, the ICHAZ of Steel B possessed the following:

1) Bulk microstructure of ferrite.

2) Little microalloy precipitation.

3) Small grain size: 20 microns (ASTM 8.5).

4) M-A constituent islands.

Other than the M-A islands, the above features are indicative of a high-toughness microstructure. The M-A islands in the ICHAZ of Steel B were potent to the extent that they reduced the toughness to the level of a CGHAZ with multiple low-toughness features. The significance of this is twofold. First, it emphasizes the toughness-reducing potential of well connected M-A islands in steel HAZs. Second, it raises questions concerning the significance of the other low-toughness features listed for CGHAZs; perhaps they are secondary factors.

It is believed that islands of high-carbon, M-A constituent, which are fairly continuous (well connected) around grain boundaries, can reduce toughness by two mechanisms (Refs. 2, 7, 8, 14, 15). They can provide microcracking initiation sites, and they can generate plastic constraint in the adjacent matrix, which reduces the ability of the matrix to resist fracture initiation. Future studies concerning the micromechanics of M-A islands will be useful in understanding and improving HAZ toughness.

#### CTOD Testing vs. Charpy Testing

The results of the present program indicate that while the CTOD technique showed a distinct difference in ICHAZ toughness between steels A and B, the Charpy method showed no difference. Also, the CTOD results for Steel B were unacceptable to most standards, while the Charpy results were acceptable. This phenomena has been reported previously for CGHAZs (Refs.1, 4).

During the CTOD test, the stress ahead of the fatigue crack tip rises quickly within a very short distance. If the crack tip is located in a low-toughness microstructure, initiation can occur before adjacent microstructures are subjected to high stress. During the Charpy test, the relatively large notch-root radius (0.25 mm/0.01 in.) causes stress to rise more gradually over a larger distance than does the fatigue crack. Before the stress becomes high enough for initiation to occur (even if the notch is located directly in a low-toughness zone), the elevated stress area spreads into adjacent HAZ regions. These regions then contribute to the energy absorption capability of the specimen.

The ICHAZ is bounded by the fine-grained HAZ and the subcritical HAZ (Figs.1, 2). For Steel B, both of these regions possessed higher toughness than the ICHAZ. It is likely that the ICHAZ Charpy results for Steel B were favorably influenced by adjacent HAZ regions. The Charpy test may be insensitive when the local microstructure varies significantly over small distances.

## Conclusions

1) During the ICHAZ thermal cycle, austenite islands form at prior pearlite colonies and ferrite grain boundaries. If the austenite has sufficient hardenability, high-carbon, M-A constituent can form upon cooling.

2) One of the steels investigated (Steel B) displayed M-A islands in the ICHAZ. The main factor influencing M-A island formation is believed to be the austenite hardenability. A combination of vanadium in solid solution in the base metal ferrite and high-silicon content was believed to be the primary factors in raising hardenability and creating the M-A constituent. The M-A islands caused low-fracture toughness, and CTOD results were in or near the linear elastic regime.

3) The ICHAZ thermal cycle does not remove all traces of base metal microstructure as does the CGHAZ thermal cycle. The steel manufacturing technique can significantly affect ICHAZ toughness.

4) By comparing low-toughness ICHAZ features with those reported for CGHAZs, it is concluded that M-A islands (if present) are a primary factor in controlling HAZ toughness.

5) Charpy testing may be insensitive in detecting low toughness when the local microstructure varies over small distances as for the case of weld HAZs in steels.

*Acknowledgment*

The authors wish to acknowledge The Welding Institute staff members who produced the weldments and the mechanical tests within the project discussed in Ref. 5.

*References*

1. Fairchild, D. P. 1987. Local brittle zones in structural welds. *Welding Metallurgy of Structural Steels.* The Metallurgical Society, Warrendale, Pa., pp. 303–318.

2. Koo, J. Y., and Ozekcin, A. 1987. Local brittle zone microstructure and toughness in structural steel weldments. *Welding Metallurgy of Structural Steels.* The Metallurgical Society, Warrendale, PA., pp 119–135.

3. Thaulow, C., Paauw, A. J., and Guttormsen, K. 1987. The heat-affected zone toughness of low-carbon microalloyed steels. *Welding Journal* 59(9):266-s to 279-s.

4. Bateson, P. H., Webster, S. E., and Walker, E. F. 1988. Assessment of HAZ toughness using small scale tests. Proc. 7th Int'l Conf. Offshore Mechanics and Arctic Engineering. Houston, Tex.

5. Harrison, P. L., and Hart, P. H. M. 1988. HAZ toughness of thick-section structural steels. Proc. Int'l. Conf. on Weld Failures. The Welding Institute, London, England, Paper 45.

6. Kim, B. C., et al., 1991. Microstructure and local brittle zone phenomena in high-strength low-alloy steel welds. *Metallurgical Transactions* A, 22A, pp. 139-149.

7. Aihara, S., and Haze, T. 1988. Influence of high-carbon martensitic island on crack-tip opening displacement value of weld heat-affected zone in HSLA steels. TMS Annual Meeting, Phoenix, Ariz.

8. Uchino, K., and Ohno, Y., 1987. A study of intercritical HAZ embrittlement in HT50 for offshore structural use. Proc. 6th Int'l. Conf. Offshore Mechanics and Arctic Engineering, Houston, Tex.

9. Fairchild, D. P., Theisen, J. D., and Royer, C. P. 1988. Philosophy and technique for assessing HAZ toughness of structural steels prior to steel production. Proc. 7th Int'l. Conf. Offshore Mechanics and Arctic Engineering, Houston, Tex.

10. United Kingdom Department of Energy. 1986. Offshore installations: guidance on design and construction. Her Majesty's Stationary Office, London, England.

11. Honeycombe, R. W. K. 1987. *Steels: Microstructure and Properties*. London, England: Edward Arnold Publishers Ltd., pp. 86–87.

12. Nippes, E. F., and Nelson, E. C. 1958. Prediction of heat-affected zone microstructures from continuous-cooling transformation data. *Welding Journal,* 37(7):289-s to 294-s.

13. Bangaru, N. V., and Sachdev, A. K. 1982. Influence of cooling rate on the microstructure and retained austenite in an intercritically annealed vanadium-containing HSLA steel. *Metallurgical Transactions* A, 13A, pp. 1899–1906.

14. Fairchild, D. P. 1990. Fracture toughness testing of weld heat-affected zones in structural steels. *Fatigue and Fracture Testing of Weldments,* ASTM STP 1058, H. I. McHenry and J. M. Potter, Eds., ASTM, Philadelphia, Pa., pp. 117–141.

15. Koo, J. Y., and Thomas, G. 1979. Metallurgical factors controlling impact properties of two-phase steels. *Scripta Metallurgica,* Vol.13, pp. 1141–1145.

# WRC Bulletin 343
# May 1989

## Destructive Examination of PVRC Weld Specimens 202, 203 and 251J

This Bulletin contains three reports:

### (1) Destructive Examination of PVRC Specimen 202 Weld Flaws by JPVRC
**By Y. Saiga**

### (2) Destructive Examination of PVRC Nozzle Weld Specimen 203 Weld Flaws by JPVRC
**By Y. Saiga**

### (3) Destructive Examination of PVRC Specimen 251J Weld Flaws
**By S. Yukawa**

The sectioning and examination of Specimens 202 and 203 were sponsored by the Nondestructive Examination Committee of the Japan Pressure Vessel Research Council. The destructive examination of Specimen 251J was performed at the General Electric Company in Schenectady, N.Y., under the sponsorship of the Subcommittee on Nondestructive Examination of Pressure Components of the Pressure Vessel Research Committee of the Welding Research Council. The price of WRC Bulletin 343 is $24.00 per copy, plus $5.00 for U.S., or $8.00 for overseas, postage and handling. Orders should be sent with payment to the Welding Research Council, Room 1301, 345 E. 47th St., New York, NY 10017.

---

# WRC Bulletin 354
# June 1990

The two papers contained in this bulletin provide definitive information concerning the elevated temperature rupture behavior of 2¼Cr-1Mo weld metals.

### (1) Failure Analysis of a Service-Exposed Hot Reheat Steam Line in a Utility Steam Plant
**By C. D. Lundin, K. K. Khan, D. Yang, S. Hilton and W. Zielke**

### (2) The Influence of Flux Composition of the Elevated Temperature Properties of Cr-Mo Submerged Arc Weldments
**By J. F. Henry, F. V. Ellis and C. D. Lundin**

The first paper gives a detailed metallurgical failure analysis of cracking in a longitudinally welded hot reheat pipe with 184,000 hours of operation at 1050°F. The second paper defines the role of the welding flux in submerged arc welding of 2¼Cr-1Mo steel.

Publication of this report was sponsored by the Steering and Technical Committees on Piping Systems of the Pressure Vessel Research Council of the Welding Research Council. The price of WRC Bulletin 354 is $50.00 per copy, plus $5.00 for U.S. and $10.00 for overseas postage and handling. Orders should be sent with payment to the Welding Research Council, 345 E. 47th St., Room 1301, New York, NY 10017.